

Clustering and Correlations at the Neutron Dripline

N.A. Orr*, F.M. Marqués†

*Laboratoire de Physique Corpusculaire, IN2P3-CNRS, ISMRA et Université de Caen,
Boulevard Maréchal Juin, 14050 Caen cedex, France*

Abstract

Some recent experimental studies of clustering and correlations within very neutron-rich light nuclei are reviewed. In particular, the development of the novel probes of neutron-neutron interferometry and Dalitz-plot analyses is presented through the example of the dissociation of the two-neutron halo system ^{14}Be . The utility of high-energy proton radiative capture is illustrated using a study of the $^6\text{He}(p,\gamma)$ reaction. A new approach to the production and detection of bound neutron clusters is also described, and the observation of events with the characteristics expected for tetra-neutrons (^4n) liberated in the breakup of ^{14}Be is discussed. The prospects for future work, including systems beyond the neutron dripline, are briefly outlined.

I. INTRODUCTION

Clustering, which has long been known to occur along the line of beta stability, also appears in exotic forms as the drip-lines are approached [1,2]. The most spatially extreme form of clustering is that exhibited by neutron haloes which appear as the ground states of very weakly bound nuclei at the limits of particle stability [3,4]. Perhaps the most intriguing

*e-mail: orr@caelav.in2p3.fr

†e-mail: marques@caelav.in2p3.fr

of the halo systems are the Borromean two-neutron halo nuclei (${}^6\text{He}$, ${}^{11}\text{Li}$, ${}^{14}\text{Be}$ and ${}^{17}\text{B}$), in which the two-body subsystems – core- n and n - n – are unbound. Such behaviour naturally gives rise to the question of the correlations between the constituents. Even in the case of the most studied of these nuclei, ${}^6\text{He}$ and ${}^{11}\text{Li}$, little is known in this respect. Here aspects of an experimental programme which has involved the development of a number of novel tools specifically aimed at studying clustering and correlations in halo and related neutron-rich systems is outlined.

In the first part of this review (section 2) the nature of these correlations is explored through the application of the techniques of interferometry and Dalitz-plot analyses to kinematically complete measurements of dissociation. In the case of breakup of a halo system, both the reaction mechanism and final state interactions (FSI) come into play. As described below, neutron-neutron interferometry and Dalitz-plot analyses exploit the FSI between the fragments in the exit channel. In a complementary approach, radiative capture – in which the outgoing photon should not be affected by FSI – has been investigated as a probe of clustering in nuclei far from stability (section 3). The example described here is that of the ${}^6\text{He}(\text{p},\gamma)$ reaction.

On a more speculative note, the production and detection of bound multineutron clusters in the breakup of very neutron-rich secondary beams is explored in section 4. This approach exploits the possibility that multineutron halo nuclei and other very neutron-rich systems contain components of the wavefunction in which the neutrons exist in a relatively compact cluster-like configuration. A method is introduced for the direct detection of neutral clusters and the results obtained from an analysis of data acquired with beams of ${}^{11}\text{Li}$ and ${}^{14}\text{Be}$ is presented.

By way of a conclusion, the prospects for future work using the techniques presented here are outlined in section 5. The possibilities for extending these studies to explore the structure of systems beyond the neutron dripline are also briefly described.

II. CORRELATIONS IN TWO-NEUTRON HALO NUCLEI

As introduced above, we have explored the spatial configuration of halo neutrons at breakup through the application of the technique of intensity interferometry; an approach first developed in their pioneering work on stellar interferometry by Hanbury-Brown and Twiss in the 1950's and 60's [5] and later extended to source size measurements in high energy collisions [6]. The principle behind the technique is as follows: when identical particles are emitted in close proximity in space-time, the wave function of relative motion is modified by the FSI and quantum statistical symmetries [7] — in the case of halo neutrons the overwhelming effect is that of the FSI [8]. Intensity interferometry relates this modification to the space-time separation of the particles at emission as a function of the four-momenta of the particles through the correlation function C_{nn} , which is defined as,

$$C_{nn}(p_1, p_2) = \frac{d^2n/dp_1 dp_2}{(dn/dp_1)(dn/dp_2)} \quad (1)$$

where the numerator is the measured two-particle distribution and the denominator the product of the independent single-particle distributions [8]. As is generally the case, the single-particle distributions have been generated via event mixing. Importantly, in the case of halo neutrons special consideration must be given to the strong residual correlations [8], whilst experimentally care needs to be taken to eliminate cross talk [11].

As a first step, measurements of breakup of ${}^6\text{He}$, ${}^{11}\text{Li}$ and ${}^{14}\text{Be}$ by a Pb target [9,10] were analysed [8] (the details of the experiment may be found in refs [9,10,8]). The choice of a high-Z target was made to privilege Coulomb induced breakup, whereby the halo neutrons may in a first approximation act as spectators and for which simultaneous emission may be expected to occur. The correlation functions derived from the data, assuming simultaneous emission, were compared to an analytical formalism based on a Gaussian source [12]. Neutron-neutron separations of $r_{nn}^{RMS} = 5.9 \pm 1.2$ fm (${}^6\text{He}$), 6.6 ± 1.5 fm (${}^{11}\text{Li}$) and 5.6 ± 1.0 fm (${}^{14}\text{Be}$) were thus extracted. These results appear to preclude any strong dineutron component in the halo wavefunctions at breakup; a result which, for ${}^6\text{He}$, is in line with the radiative capture

study reported in the following section. It is interesting in this context to compare these results to the RMS neutron-proton separation of 3.8 fm in the deuteron (the only bound two nucleon system). The same analysis has been applied to dissociation of ^{14}Be by a C target, in order to investigate the influence of the reaction mechanism [14]. A result which hints at a somewhat larger separation, $r_{nn}^{rms} = 7.6 \pm 1.7$ fm, was obtained. This raises the question as to whether simultaneous emission can be assumed a priori. In principle, the analysis of the correlation function in two dimensions, transverse and parallel to the total momentum of the pair, would allow for the unfolding of the source size and lifetime [12]. Such an analysis requires a much larger data set than presently available. The two-neutron halo, however, is far less complex than the systems usually studied via interferometry (for example, heavy-ion collisions [7]). Moreover, the simple three-body nature of the system breaking up suggests that any delay in the emission of one of the neutrons will arise from core- n FSI/resonances in the exit channel, a process that may be expected to be enhanced for nuclear induced breakup.

Correlations in three-particle decays are commonly encountered in particle physics and are typically analysed using plots of the squared invariant masses of particle pairs (M_{ij}^2, M_{ik}^2), with $M_{ij}^2 = (p_i + p_j)^2$; a technique developed by the Australian physicist Richard Dalitz in the early 1950's [15,16]. In Dalitz-plot representations, FSI or resonances lead to a non-uniform population of the surface within the kinematic boundary defined by energy-momentum conservation and the decay energy. In the present case, the core- n - n system exhibits a distribution of decay energies (E_d). The E_d associated with each event will thus lead to a different kinematic boundary, and the resulting plot containing all events cannot be easily interpreted. A normalised invariant mass has thus been introduced [14],

$$m_{ij}^2 = \frac{M_{ij}^2 - (m_i + m_j)^2}{(m_i + m_j + E_d)^2 - (m_i + m_j)^2} \quad (2)$$

which ranges between 0 and 1 (that is, a relative energy $E_{ij} = M_{ij} - m_i - m_j$ between 0 and E_d) for all events and exhibits a single kinematic boundary. Examples of how n - n and core- n FSI may manifest themselves in the Dalitz plot for the decay of ^{14}Be are illustrated in

Fig. 2, whereby events have been simulated according to the simple interacting phase-space model described in ref. [14]. The inputs were an E_d distribution following that measured [10], the C_{nn} obtained with the C target, and a core- n resonance with $\Gamma = 0.3$ MeV at $E_0 = 0.8$ MeV. Note that due to the normalisation the (squared) core-neutron invariant mass does not present a simple structure directly related to the energy of the resonance/FSI [14].

The Dalitz plot for the data from the dissociation by Pb (Fig. 3, upper panel) presents a strong n - n FSI and a uniform density for $m_{nn}^2 > \sim 0.5$. Indeed, the n - n FSI alone describes very well the projections onto both axes, and therefore suggests that core- n resonances are not present to any significant extent. This result confirms the hypothesis of simultaneous n - n emission employed, as described above, in the original analysis of the dissociation of ^{14}Be by Pb [8]. The r_{nn}^{RMS} so extracted, 5.6 ± 1.0 fm, may thus be considered to represent the n - n separation in the halo of ^{14}Be .

For dissociation by the C target (Fig. 3, lower panel), despite the lower statistics, two differences are evident. Firstly, the n - n signal is weaker, indicating that a significant delay has occurred between the emission of each neutron. Second, and more importantly, the agreement between the model including only the n - n FSI and the data for m_{cn}^2 is rather poor. In order to verify whether this disagreement corresponds to the presence of core- n resonances, the core- n relative energy (E_{cn}) has been explored. It has been reconstructed for the simulations incorporating only the n - n FSI and compared in Fig. 4 to the data (the model calculations have been normalized to the data above 4 MeV). For dissociation by Pb, the inclusion of only the n - n FSI provides a very good description of the data, with the exception of small deviations below 1 MeV. This is in line with the Dalitz-plot analysis discussed above.

The deviations observed for the C target between the measured m_{cn}^2 and the simulation including only the n - n FSI clearly correspond to structures in the E_{cn} spectrum. Moreover, these structures are located at energies that are in line with those of states previously reported in ^{13}Be : the supposed $d_{5/2}$ resonance at 2.0 MeV [17–19,21] and a lower-lying

state(s) [18–21]. The model-to-data ratio is about 1/2, indicating that the peaks correspond to resonances formed by one of the neutrons in almost all decays; the solid line accounts for the contribution of the neutron not interacting with the core. If we add to the phase-space model with n - n FSI core- n resonances ($\Gamma = 0.3$ MeV) at $E_0 = 0.8, 2.0$ and 3.5 MeV with intensities of 45, 35 and 20%, respectively, the data are well reproduced (dashed line). In the case of dissociation by Pb, the lowest-lying level(s) appears to be present in at most 10% of events.

In the context of the influence of the reaction mechanism, it is worthwhile noting that whilst some 35% of the two-neutron removal cross section on the Pb target is attributable to nuclear induced breakup [10], the requirement of two neutrons in coincidence with the ^{12}Be core in the present analysis reduces this to some 15% – approximately half of the two-neutron removal cross section arises from absorption.

By combining the information extracted from the core- n channel with the n - n correlation functions, the analysis can be extended to extract the average lifetime of the core- n resonances. If the n - n separation in ^{14}Be is fixed to that obtained for dissociation by Pb, $r_{nn}^{RMS} = 5.6 \pm 1.0$ fm, the delay between the emission of the neutrons τ_{nn} needed to describe the n - n correlation function for the C target may be introduced. As discussed above, this delay should correspond to the lifetime of the resonances. The result of a χ^2 analysis, represented by the dashed lines in Fig. 4 (bottom right panel), suggests an average lifetime of 150^{+250}_{-150} fm/ c .

III. RADIATIVE PROTON CAPTURE AS A PROBE OF CLUSTERING

In a recent investigation of coherent bremsstrahlung production in the reaction $\alpha(p, \gamma)$ it was demonstrated that the high-energy photon spectrum is dominated by capture to form ^5Li [22]. This result provided the motivation to extend the technique to probe clustering in more exotic systems [23]. As a first test ^6He was chosen owing to the relatively high beam intensities available and the fact that structurally it is the most well established two-

neutron halo nucleus. Given a proton wavelength of 0.7 fm at 40 MeV, direct capture might be observed, as a quasi-free process, on the constituents (α - n - n) of ${}^6\text{He}$ in addition to capture into ${}^7\text{Li}$. Moreover, the different quasi-free capture (QFC) processes would lead to different E_γ in the range 20–40 MeV.

Experimentally, a 40 MeV/nucleon ${}^6\text{He}$ beam (5×10^5 pps) was employed to bombard a solid hydrogen target (95 mg/cm^2). The different charged reaction products were identified and momentum analysed using the SPEG spectrometer. The photons were detected using 74 elements of the “Château de Cristal” BaF_2 array, with a total efficiency of some 70%. Further details including the analysis techniques may be found in ref. [23].

Turning to the experimental observations, the reaction ${}^6\text{He}(p,\gamma){}^7\text{Li}$ is unambiguously identified by the γ -rays in coincidence with ${}^7\text{Li}$ (Fig. 5). In particular, the photon energy spectrum, as well as the ${}^7\text{Li}$ momentum [23], is well described assuming a γ -ray line at 42 MeV. The energy difference between the two particle-stable states of ${}^7\text{Li}$ – the g.s. and the first excited state at 0.48 MeV) – is too small for them to be distinguished in this experiment. A total cross section of $\sigma = 35 \pm 2 \mu\text{b}$ was deduced.

The ${}^6\text{He}(p,\gamma){}^7\text{Li}$ cross section has been calculated using a microscopic cluster model [25]. At 40 MeV, a cross section of $\sigma = 59 \mu\text{b}$ was found, with $15\mu\text{b}$ going to the g.s. and $44\mu\text{b}$ to the first excited state [23]. The calculation was restricted to the dominant E1 multipolarity, thus leading to an angular distribution symmetric about 90° (Fig. 5b). The cross section to the g.s. can also be estimated from photodisintegration measurements [27] via detailed balance considerations and is $9.6 \pm 0.4 \mu\text{b}$. Given the predicted relative populations of the ground and first excited state, a total capture cross section of $\sigma \sim 38 \mu\text{b}$ is obtained, in agreement with the value measured here.

QFC was investigated by searching for γ -rays in coincidence with fragments lighter than ${}^7\text{Li}$. The corresponding energy spectra (Fig. 6a,c,e) do indeed exhibit peaks below 42 MeV. In order to establish the origin of these fragment- γ coincidences, QFC processes on the subsystems of ${}^6\text{He}$ have been modelled as follows. The ${}^6\text{He}$ projectile was considered as a cluster (A) plus spectator (a) system in which each component has an intrinsic momentum

distribution, the corresponding energy $E_A + E_a - m_{\text{He}}$ being taken into account in the total available energy. The reaction may be denoted as $a + A(p, \gamma) B + a$, and the γ -ray angular distribution is assumed to be that given by the charge asymmetry of the entrance channel [24]. The intrinsic momentum distribution of all the clusters was taken to be Gaussian in form (FWHM = 80 MeV/c). In order to explore the possibility that FSI may occur in the exit channel between the spectator, a , and the capture fragment, B , an extended version of the QFC calculation was developed [23]. Here the energy in the system $B + a$ is treated as an excitation in the continuum of ${}^7\text{Li}$, which decays in flight.

In the case of ${}^6\text{Li}$ - γ coincidences, two lines were observed (Fig. 6a) at 30 and 3.56 MeV corresponding to the formation of ${}^6\text{Li}$ and the decay of the second excited state. It was estimated that ${}^6\text{Li}$ is formed almost exclusively ($96^{+4}_{-24}\%$) in the 3.56 MeV excited state. The deduced cross section was $\sigma = 3.5 \pm 1.3 \mu\text{b}$. The lines in Fig. 6a,b corresponds to QFC on ${}^5\text{He}$ into ${}^6\text{Li}^*(3.56 \text{ MeV})$. The γ -ray energy spectrum is well described, whilst the ${}^6\text{Li}$ momentum distribution requires inclusion of ${}^6\text{Li}$ -n FSI.

Evidence for QFC on the α core, whereby the two halo neutrons would behave as spectators, has also been searched for. The photon spectrum should resemble that observed for the $\alpha + p$ reaction [22]. Indeed such a γ -ray energy spectrum (Fig. 6c) was observed. The background, however, arising from ${}^6\text{He}$ breakup, in which the α particle is detected in SPEG and the halo neutrons interact with the forward-angle detectors of the Château, is significant. In order to minimise this background, only the backward-angle detectors ($\theta > 110^\circ$) of the Château were used in the analysis. The γ -ray spectrum under this condition exhibits two components: a peak at $E_\gamma = 27 \text{ MeV}$ and a $1/E_\gamma$ continuum similar to coherent $\alpha + p$ bremsstrahlung [22].

Simulations indicate, however, that some back-scattered neutrons remain from breakup, which would also lead to a continuous component with a $1/E$ type spectrum in the Château [23]. A single background component of this form (dotted line, Fig. 6c) was therefore added to the QFC process $\alpha(p, \gamma){}^5\text{Li}$. The photon energy spectrum is thus well described, as is the momentum distribution of the α particle. The cross section was estimated to be $\sigma = 4 \pm 1 \mu\text{b}$.

Additional support for this interpretation is found in α - γ -n coincidences, for which 30 events were observed [23] (open symbols, Fig. 6c).

Finally, d- γ coincidences presenting a peak in the γ -ray energy spectrum, at $E_\gamma \simeq 21$ MeV, were also observed (Fig. 6e). The relatively low statistics arose from the limited acceptances of the spectrometer for deuterons (Fig. 6f). The predictions for n(p, γ)d QFC on a halo neutron present a peak at 19 MeV (Fig. 6e) – the small shift may be attributable to the strong kinematic correlation between the deuteron momentum and the photon energy, as the detection of only a small fraction of the deuterons is predicted [23]. As such no reliable estimate of the cross section was possible.

There are additional QFC channels, $2n(p,\gamma)t$ and $t(p,\gamma)\alpha$, that could have been observed with finite efficiency but were not [23]. Perhaps the most interesting is QFC on the two halo neutrons. In the case of ${}^6\text{He}$, several theoretical models predict the coexistence of two configurations in the g.s. wave function: the so-called “di-neutron” and “cigar” configurations [28]. Here one might expect that the different admixtures of these could be probed by the relative strength of the n, $2n(p,\gamma)d,t$ QFC processes, whereby the corresponding free cross sections at 40 MeV, obtained from detailed balance considerations, are comparable: $9.6\mu\text{b}$ [29] and $9.8\mu\text{b}$ [30], respectively. However, events registered in the Château in coincidence with tritons in SPEG have energies below 10 MeV, whereas the $2n(p,\gamma)t$ reaction should produce photons with $E_\gamma \approx 32$ MeV.

As described above, the QFC with fragment FSI model describes well the observed monoenergetic γ -rays, as well as the momentum distribution of the capture fragment (B). The γ -ray lines are associated with specific energy distributions for the fragments in the exit channel. Therefore, such a process will exhibit the same kinematics as capture into continuum states above the corresponding threshold, ${}^6\text{He}(p,\gamma){}^7\text{Li}^* \rightarrow B + a$, provided that the equivalent region of the continuum is populated [23]. If, however, all the final states observed here were the result of radiative capture into ${}^7\text{Li}$, capture via the non-resonant continuum in ${}^7\text{Li}$ might well be expected to occur [31]. This would lead to a continuous component to the γ -ray energy spectra. Moreover, events corresponding to $E_{7\text{Li}^*} = 0.5\text{--}10$ MeV have

not been observed in either t - γ coincidences or α - γ coincidences with $E_\gamma = 32$ – 42 MeV, nor has the decay into $\alpha+t$ for $E_{7\text{Li}^*} > 10$ MeV. Within the picture of QFC on clusters, this is simply explained by the absence of the $2n(p,\gamma)t$ and $t(p,\gamma)\alpha$ QFC processes for the ${}^4\text{He}$ - $2n$ and t - t configurations, respectively. This indicates, as suggested by the interferometry measurements described in the previous section, that ${}^4\text{He}$ - n - n (i.e., no compact dineutron component) is the dominant configuration present in ${}^6\text{He}_{gs}$.

IV. MULTINEUTRON CLUSTERS

The very lightest nuclei have long played a fundamental rôle in testing nuclear models and the underlying nucleon-nucleon interaction. In this context the study of systems exhibiting very asymmetric N/Z ratios may provide new perspectives on the nucleon-nucleon interaction and few-body forces. In the case of the light, two-neutron halo nuclei such as ${}^6\text{He}$, insight is already being gained into the effects of the three-body force [28]. Very recently evidence has been presented that the ground state of ${}^5\text{H}$ exists as a relatively narrow, low-lying resonance [32]. In the case of the lightest $N = 4$ isotone, 4n , nothing is known despite experimental searches over the past 40 years [33,34]. Theoretically it is difficult to produce a bound 4 neutron cluster (or “tetra-neutron”) [33,35–38]. The discovery of such neutral systems as bound states would therefore, as discussed by Timofeyuk [35] and Pieper [38], have fundamental implications for our understanding of nuclear forces.

It is, therefore, interesting to speculate that multineutron halo nuclei and other very neutron-rich systems may contain components of the wavefunction in which the neutrons present a relatively compact cluster-like configuration. If this were to be the case, then the dissociation of beams of such nuclei may offer a means to produce bound neutron clusters (if they exist) and, more generally study multineutron correlations.

To date the majority of searches for multineutron systems have relied on very low (typically ~ 1 nb) cross section double-pion charge exchange ($D\pi\text{CX}$) and heavy-ion transfer reactions (see, for example, refs [39,40]). In the case of dissociation of an energetic beam of

a very neutron-rich nucleus, relatively high cross sections (typically ~ 100 mb) are encountered. Thus, even only a small component of the wavefunction corresponding to a multineutron cluster could result in a measurable yield with a moderate secondary beam intensity. Furthermore the backgrounds arising in $D\pi CX$ and heavy-ion transfer reactions from target impurities and complex many-body phase space reactions are obviated in breakup.

The difficulty in this approach lies in the direct detection of a $^A n$ cluster. The avenue that has been explored here¹ is to detect the recoiling proton in a liquid scintillator [42]. One of the principle advantages of a liquid scintillator is that neutrons may be discriminated with good efficiency from the γ and cosmic-ray backgrounds using pulse-shape analysis. Careful calibrations, employing sources, cosmic rays and the maximum proton recoil energy for a given E_n , permit the charge deposited and hence the energy (E_p) of the recoiling proton to be determined. This may be compared to the energy derived from the measured time-of-flight (E_n): for a single neutron and an ideal detector, $E_p/E_n \leq 1$; for a realistic detector with finite resolution the limit is ~ 1.4 . In the case of a multineutron cluster ($^A n$) E_p can exceed the incident energy per nucleon and E_p/E_n will take on a range of values extending beyond 1.4 — up to ~ 3 in the case of $A=4$ (Fig. 7).

The data already at hand from the study of the dissociation of ^{14}Be and ^{11}Li [8,10,14] was examined with a view to testing the method outlined above. The details of the analyses carried out may be found in ref. [42]. The essential results are provided by figures 8 and 9 which display the charged fragment particle identification (PID) derived from the Si-CsI detector telescope versus E_p/E_n . The E_p/E_n distributions (upper panels in Figs. 8 and 9) exhibit a general trend below 1.4: a plateau up to 1 followed by a sharp decline, which may be fitted to an exponential distribution (dashed line). In the region where $^A n$ events may

¹Those with an historical inclination will recognise the method as similar in principle to that employed by Chadwick [41] in discovering the neutron (thus supporting the view sometimes held by one of the authors that there is nothing truly new in nuclear structure physics).

be expected to appear some 7 events with E_p/E_n ranging from 1.4 to 2.2 are observed for ^{14}Be . In the case of ^{11}Li , despite the greater number of neutrons detected (factor of 2.4), only 4 events appear which lie just above threshold. Turning to the coincidences with the charged fragments, the 7 events produced by the ^{14}Be beam fall within a region centred on ^{10}Be . In the case of the 4 events produced in the reactions with ^{11}Li no correlation appears to exist with any particular fragment.

The left panel in figure 10 displays in more detail the region of the particle identification spectrum for the breakup of ^{14}Be into lighter Be isotopes, together with the 7 events in question. Clearly the resolution in PID does not allow the observed events to be unambiguously associated with a ^{10}Be fragment. However, the much higher cross-section for this channel (460 ± 40 mb) compared to ^{11}Be (145 ± 20 mb) suggests that this may be the case. It should be noted that the PID is somewhat complicated by the fact that reactions also occur in the Si-CsI telescope. The effects of this are shown in figure 10 (right panel), whereby the reactions in the telescope give rise to a tail extending to higher mass Be fragments. A dedicated experiment including a high statistics target-out measurement, or ideally using a large acceptance sweeper magnet, would eliminate this ambiguity.

As a first step towards investigating the nature of the events with $E_p/E_n > 1.4$ each was examined to verify that it corresponded to a well defined event in both the charged particle and neutron detectors. Of the 7 events observed in the breakup of ^{14}Be , all but one survived. The 6 remaining events thus appear to exhibit characteristics consistent with detection of a multineutron cluster from the breakup of ^{14}Be . Potential sources of such events not involving the formation of a multineutron were consequently examined [42].

The most obvious source of events that may mimic a multineutron cluster is the detection, in the same event, of more than one neutron in the same module. The rates at which such pile-up is expected to occur have been examined in detail employing both simulations which reproduce the observed neutron angular, energy and multiplicity distributions, together with an analysis based on the measured neutron-neutron relative angle distributions [42]. As summarised in Table 1, the two methods provide consistent results which are in line

with the numbers of events observed for the channels ($^{11}\text{Li}, \text{X}+\text{n}$) and ($^{14}\text{Be}, ^{12}\text{Be}+\text{n}$). In the case of ($^{14}\text{Be}, ^{10}\text{Be}$), less than one event arising from pile-up is estimated to occur with $E_p/E_n > 1.4$, compared to some 6 observed events. It may be concluded, therefore, that a signal consistent with the production of a multineutron cluster in the breakup of ^{14}Be – most probably in the channel $^{10}\text{Be}+^4\text{n}$ – has been observed at a level some 2-sigma above that attributable to background processes.

The average flight time of the 6 events from the target to the neutron array is ~ 100 ns. Unless the decay of the 4 neutron system takes place via the emission of highly correlated neutrons, the lifetime of the putative tetra-neutron is of this order or longer; suggesting a particle bound system or a very narrow resonance. The conditions applied in the analysis make an estimate of the production cross-section rather difficult. Nonetheless, if it is assumed that these conditions affect the number of neutrons and ^4n events in a similar manner, the cross-section measured for the production of ^{10}Be [10] may be scaled by the relative yields, resulting in a cross section $\sigma(^4\text{n}) \sim 1$ mb.

V. CONCLUSIONS

An experimental programme to explore clustering and correlations in halo and related neutron-rich systems has been reviewed. New approaches have been described, including the application of neutron-neutron interferometry and Dalitz-plot analyses to the dissociation of two-neutron halo nuclei and the investigation of radiative capture as a probe of clustering. The use of these techniques to study very proton-rich nuclei is clearly feasible, if somewhat complicated by the addition of Coulomb effects.

Present work is concentrating on a high statistics measurement of the dissociation of ^6He [43]. Given that ^6He is structurally the most well known two-neutron halo system, this should provide a good test of the methods described here to probe correlations. Furthermore, correlation function analyses employing the longitudinal and transverse neutron-neutron relative momenta [12] should provide an independent means to disentangle the halo neutron-neutron

separation and time delay in emission. Measurements completed very recently employing a ^8He beam provided by the SPIRAL facility at GANIL should permit multineutron correlations to be explored [43].

Turning to more exotic systems, the study of the structure of nuclei beyond the neutron dripline has attracted renewed attention in recent years (see, for example, [32,44–47]). Beyond the core–valence neutron(s) correlations, which will manifest their presence as resonances or virtual states, strong correlations may, as suggested by Seth and Parker [48] and Jensen and Riisager [49], persist between the neutrons. As a first step towards exploring these ideas, high-energy single-proton removal reactions² with beams of ^6He [50] (Fig. 11b), ^{14}B [21] and ^{17}C [21] (Fig. 11a) have been measured. In the case of $t + n + n$ (Fig. 11b), a structure similar in energy and width to that attributed previously [32] to ^5H is observed. Despite the limited statistics, a preliminary Dalitz-plot analysis indicates the presence of significant n - n correlations.

As described in section 3, a number of different reaction channels were observed in the radiative capture study. Beyond $^6\text{He}(p,\gamma)^7\text{Li}$, evidence for quasifree capture on ^5He , α and n was found. Of particular importance was the observation of events which correspond to the previously measured $\alpha(p,\gamma)$ reaction, as well as the non-observation of capture on a dineutron. Theoretically, models need to be developed to describe capture on the constituent clusters of exotic nuclei and, for comparison, capture on the projectile into unbound final states. In the future, the advent of intense ^8He beams may allow α - $4n$ and ^6He - $2n$ configurations to be probed. Comparison with the recent breakup reaction study should prove illuminating.

In terms of neutron clusters the confirmation or otherwise of the events observed here with a higher intensity ^{14}Be beam and improved fragment detection system is essential [51]. The

²Such reactions are of considerable spectroscopic interest as the neutron configuration of the projectile remains essentially unperturbed [21,46].

search for similar events in the breakup of ^8He is currently underway as part of the breakup study noted above. Importantly, in tandem with this experiment, a complementary study employing the $d(^8\text{He}, ^6\text{Li})^4\text{n}$ transfer reaction, which should be sensitive to both bound and resonant states of the ^4n , was carried out [52] (unfortunately such a transfer reaction study of the ^4n system with a ^{14}Be beam is not feasible). Searches employing other reactions such as knockout – $^8\text{He}(p, p\alpha)^4\text{n}$ with detection of the ^4n and/or the proton and α – are also to be encouraged.

We would like to draw special attention to the key rôles played by Marc Labiche (^{14}Be breakup) and Emmanuel Sauvan (radiative capture) in the work described here. It is also a pleasure to thank the members of the E295,332,378 and 415 collaborations and, in particular, the DEMON and CHARISSA teams for their contributions. The support provided by the technical staffs of LPC and GANIL (LISE, SPEG and cyclotron operations crews) in preparing and executing the experiments is gratefully acknowledged. This work was funded under the auspices of the IN2P3-CNRS (France), EPSRC (United Kingdom) et FNRS (Belgique). Additional support from the ALLIANCE programme (Ministère des Affaires Etrangères and British Council) and the Human Capital and Mobility Programme of the European Community (Access to Large Scale Facilities) is also acknowledged.

TABLES

TABLE I. Comparison of the number of events observed (exp) with $E_p/E_n > 1.4$ for each channel with the estimated number of events expected from pile-up. The methods are based on a Monte-Carlo simulation (sim), and the measured relative-angle distribution of n - n pairs (nn). The latter is quoted in terms of a conservative upper limit [42].

Channel	N_{2n}^{exp}	$N_{2n}^{(\text{sim})}$	$N_{2n}^{(\text{nn})}$
($^{11}\text{Li}, \text{X}$)	4	~ 3	< 7.0
($^{14}\text{Be}, ^{12}\text{Be}$)	0	0.8	< 1.2
($^{14}\text{Be}, ^{10}\text{Be}$)	6	0.2	< 0.8

REFERENCES

- [1] W. von Oertzen, H.G. Bohlen, “Covalently Bound Molecular States in Beryllium and Carbon Isotopes”, contribution to this volume.
- [2] M. Freer, “Molecules in Nuclei”, contribution to this volume.
- [3] I. Tanihata, “Halo Nuclei”, contribution to this volume.
- [4] F.M. Nunes, “Probing the Halo Structure”, contribution to this volume.
- [5] R. Hanbury-Brown, R. Twiss, *Philos. Mag.* **45** (1954) 663
- [6] G. Goldhaber *et al.*, *Phys. Rev.* **120** (1960) 300
- [7] D.H. Boal *et al.*, *Rev. Mod. Phys.* **62** (1990) 553
- [8] F.M. Marqués *et al.*, *Phys. Lett.* **B476** (2000) 219
- [9] N.A. Orr *et al.*, “Reaction Study of the Two-Neutron Halo Nucleus ^{14}Be ”, GANIL Proposal E295, February 1997
- [10] M. Labiche *et al.*, *Phys. Rev. Lett.* **86** (2001) 600;
M Labiche, “Etude de la dissociation du ^{14}Be , noyau Borroméen à halo de deux neutrons”, Thèse, Université de Caen, (1999), LPCC T 99-03
- [11] F.M. Marqués *et al.*, *Nucl. Inst. Meth.* **A450** (2000) 109
- [12] R. Lednicky, L. Lyuboshits, *Sov. J. Nucl. Phys.* **35** (1982) 770
- [13] N.A. Orr, *Eur. Phys. J.* **A15** (2002) 109
- [14] F.M. Marqués *et al.*, *Phys. Rev.* **C64** (2001) 061301R
- [15] R.H. Dalitz, *Philos. Mag.* **44** (1953) 1068
- [16] D.H. Perkins, “Introduction to High Energy Physics”, Addison Wesley (Menlo Park, California, 1987) Chapter 4

- [17] A.N. Ostrowski *et al.*, Z. Phys. **A343** (1992) 489
- [18] A.V. Belozyorov *et al.*, Nucl. Phys. **A636** 419 (1998) 419
- [19] K.L. Jones, “The Unbound Nucleus ^{13}Be ”, Thesis, University of Surrey (2001);
N.A. Orr, nucl-ex/0011002 and refs therein;
H. Simon, “Aufbruchreaktionen der Halokerne ^{11}Li und ^{14}Be bei Relativistischen Energien”, Thesis , Technical University of Darmstadt (1998);
H. Simon *et al.*, in preparation
- [20] M. Thoennessen *et al.*, Phys. Rev. **C63** 014308 (2001) 014308
- [21] J.L. Lecouey, “Etudes des Systèmes Non Liés ^{13}Be et ^{16}B ”, Thèse, Université de Caen (2002), LPC Rapport LPCC T 02-03
- [22] M. Hoefman *et al.*, Phys. Rev. Lett. **85** (2000) 1404
- [23] E. Sauvan *et al.*, Phys. Rev. Lett. **87** (2001) 042501
E. Sauvan, “Etude de la structure de noyaux riches en neutrons à l’aide de nouvelles sondes”, Thèse, Université de Caen, LPCC T-00-01 (2000)
- [24] M. Hoefman *et al.*, Nucl. Phys. A **654** (1999) 779c
- [25] P. Descouvemont, Nucl. Phys. A **584** (1995) 532
- [26] H.R. Weller *et al.*, Phys. Rev. C **25** (1982) 2921
- [27] M.R. Sené *et al.*, Nucl. Phys. A **442** (1985) 215
- [28] M.V. Zhukov *et al.*, Phys. Rep. **231** (1993) 151
- [29] J. Ahrens *et al.*, Phys. Lett. **52B** (1974) 49
- [30] D.D. Faul *et al.*, Phys. Rev. Lett. **44** (1980) 129
- [31] S.A. Siddiqui, N. Dytlewski, H.H. Thies, Nucl. Phys. A **458**, 387 (1986)

- [32] A.A. Korshennikov *et al.*, Phys. Rev. Lett. **87** (2001) 092501
- [33] D.R. Tilley, H.R. Weller, G.M. Hale, Nucl. Phys. **A541** (1992) 1 and references therein
- [34] A.A. Ogloblin, Y.E. Penionzhkevich, in *Treatise on Heavy-Ion Science (vol. 8): Nuclei Far From Stability*, ed. D.A. Bromley (Plenum Press, New York, 1989) p 261 and references therein
- [35] N. Timofeyuk, J. Phys. **G29** (2003) L9; nucl-th/0301020
- [36] C. Bertulani, V. Zelevinsky, nucl-th/0212060
- [37] J. Carbonell, *priv. comm.*
- [38] S.C. Pieper, nucl-th/0302048
- [39] J. Grüter *et al.*, Eur. Phys. J. **4** (1999) 5
- [40] H.G. Bohlen *et al.*, Nucl. Phys. **A583** (1995) 775
- [41] J. Chadwick, Nature **129** (1932) 312
- [42] F.M. Marqués *et al.*, Phys. Rev. **C65** (2002) 044006
- [43] F.M. Marqués, F. Hanappe *et al.*, “Multi-particle Correlations and the Structure of Heavy He Isotopes”, GANIL Proposal E378, September 2000
- [44] A.A. Korshennikov *et al.*, Phys. Lett. **B326** (1994) 31;
A.N. Ostrowski *et al.*, Phys. Lett. **B338** (1994) 13
- [45] A.A. Korshennikov *et al.*, Phys. Rev. Lett. **82** (1999) 3581
- [46] L. Chen *et al.*, Phys. Lett. **B505** (2001) 21
- [47] M. Meister *et al.*, Phys. Rev. Lett. **88** (2002) 102501;
H.G. Bohlen *et al.*, Phys. Rev. **C64** (2001) 024312
- [48] K.K. Seth, B. Parker, Phys. Rev. Lett. **66** (1991) 2448

- [49] A.S. Jensen, K. Riisager, Phys. Lett. **B264** (1991) 238
- [50] G. Normand, unpublished
- [51] F.M. Marqués, F. Hanappe *et al.*, “Search for Multineutrons and Correlations in the Breakup of ^{14}Be ”, GANIL Proposal E415, March 2002
- [52] D. Beaumel, R. Wolski *et al.*, “Study of the 4-Neutron System using the $d(^6\text{He}, ^6\text{Li})$ Reaction”, GANIL Proposal E422S, March 2002

FIGURES

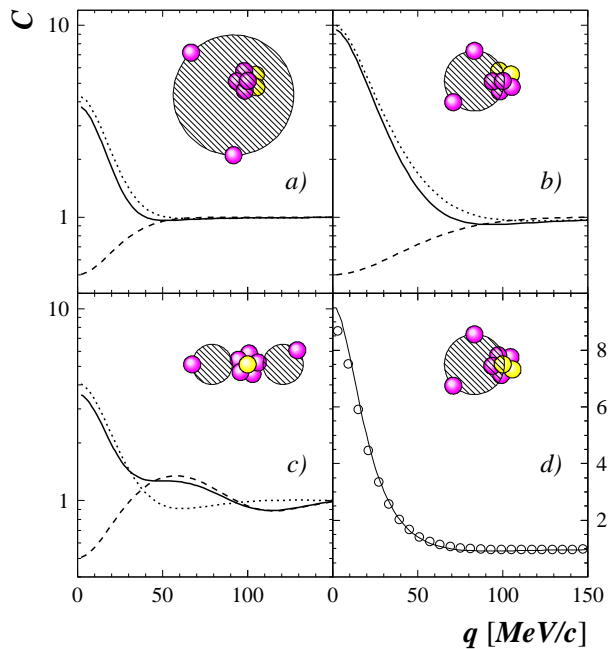


FIG. 1. Neutron-neutron correlation functions, C , for different halo configurations. The calculations are based on Gaussian sources with sizes, σ , of (a) 6 fm, (b) 3 fm and (c) 2 fm separated by 10 fm. The contributions from Fermi-Dirac statistics and the neutron-neutron FSI are shown by the dashed and dotted lines respectively. The simultaneous emission for a source size of 3 fm (solid line) is compared in (d) to a space-time extent of 3 fm, 50 fm/c (open symbols) [8].

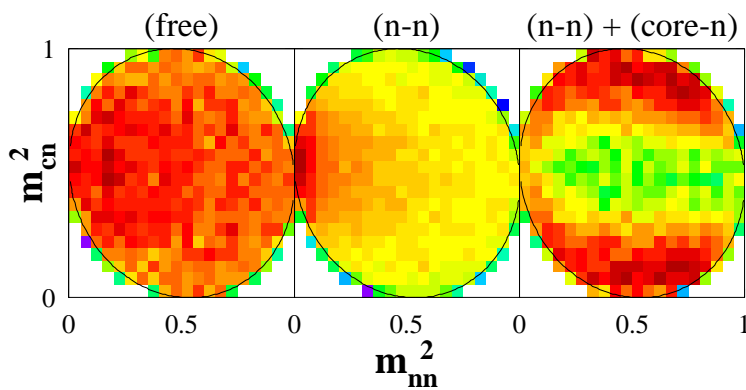


FIG. 2. Dalitz plot for the simulated decay of ^{14}Be (see text). In the left panel no FSI are included. From ref. [13].

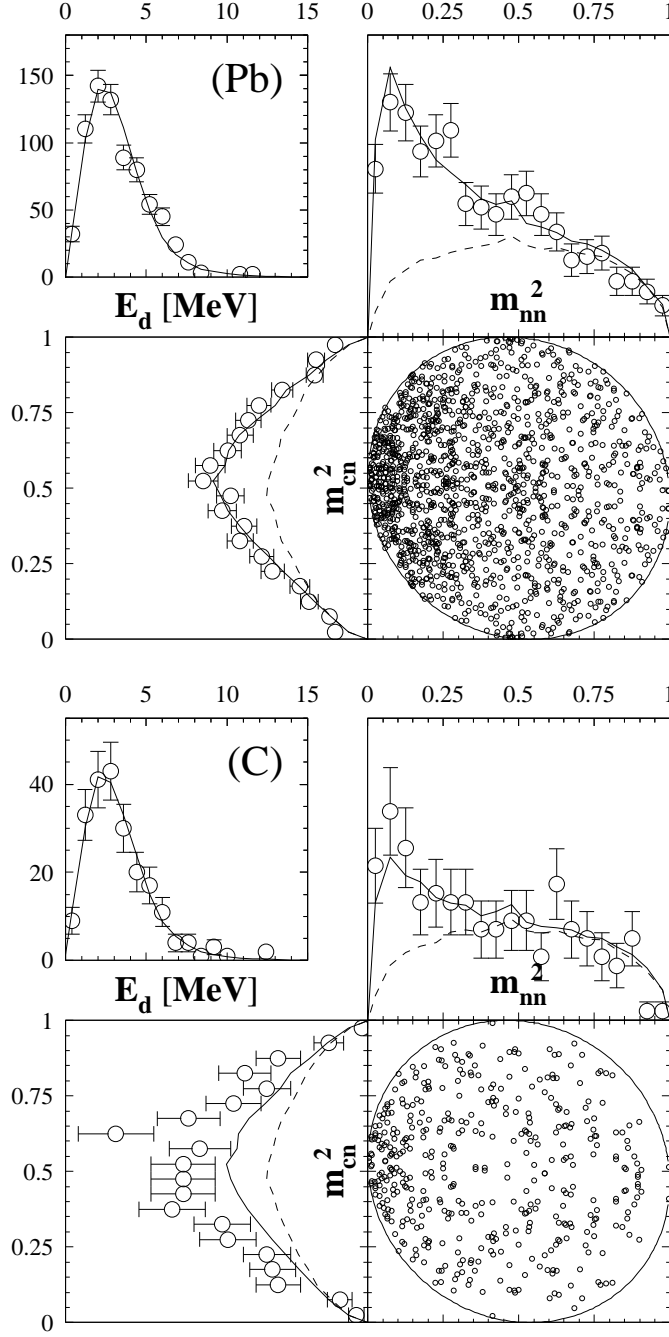


FIG. 3. Dalitz plot and the projections onto the squared invariant masses for the dissociation of ^{14}Be by Pb (upper) and by C (lower panels). The lines are the phase-space model simulations with/without (solid/dashed) n - n FSI. The inset shows the measured E_d spectrum. From ref. [14]

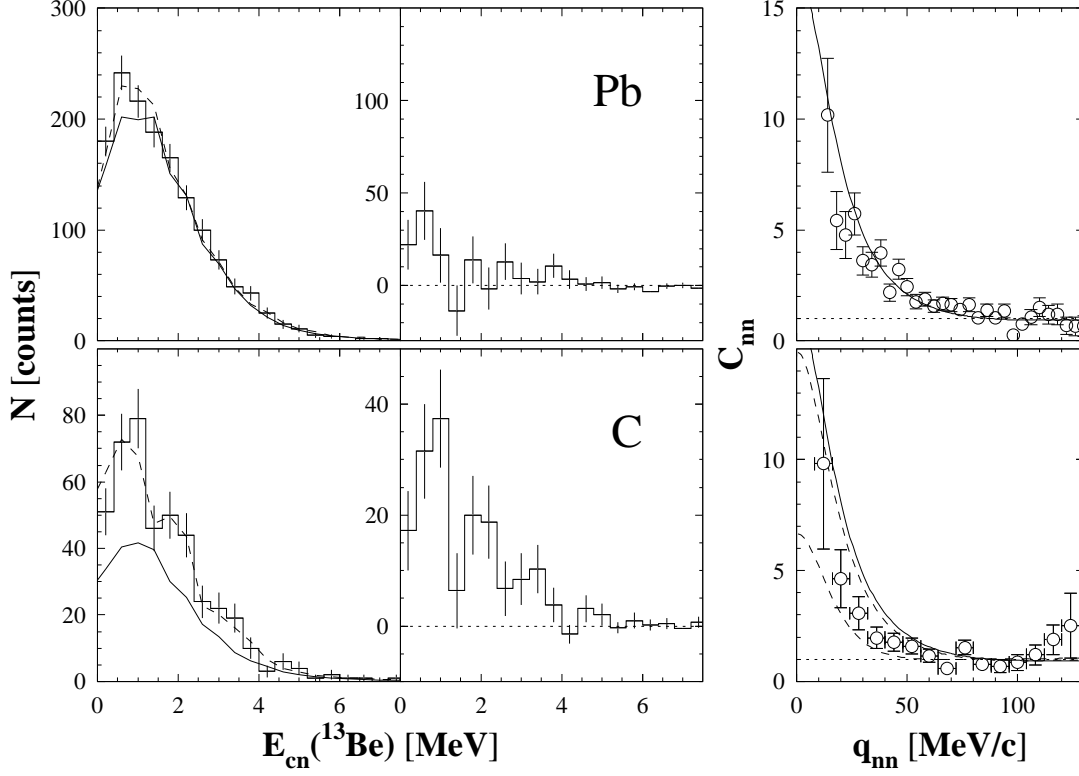


FIG. 4. Core- n relative energy distributions (left) and n - n correlation functions (rightmost panels) for the dissociation of ^{14}Be by Pb and C. The lines in the E_{cn} spectra are the result of the phase-space model simulations with n - n FSI (solid) plus core- n FSI (dashed, see text). The histograms presented in the middle panels are the difference between the data and the n - n FSI simulations. The solid lines in the panels at the right are the C_{nn} for $r_{nn}^{RMS} = 5.6$ fm and $\tau_{nn} = 0$; the dashed lines correspond to the limits of the range $r_{nn}^{RMS} = 6.6$ – 4.6 fm and $\tau_{nn} = 0$ – 400 fm/c. From ref. [14].

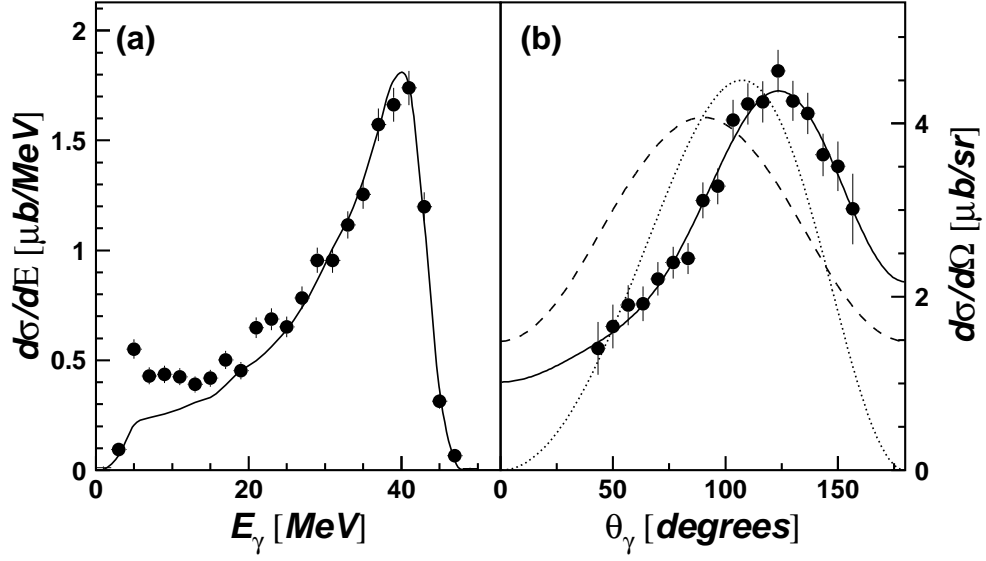


FIG. 5. Energy (a) and angular distributions (b) in the ${}^6\text{He}+p$ c.m. for photons in coincidence with ${}^7\text{Li}$. The solid line in (a) is the response of the Chateau to $E_\gamma = 42$ MeV. The lines in (b) are a classical electrodynamics calculation [24] (dotted), a cluster model [23,25] (dashed), both normalized to the data, and a Legendre polynomial fit [26] (solid). From ref. [23]

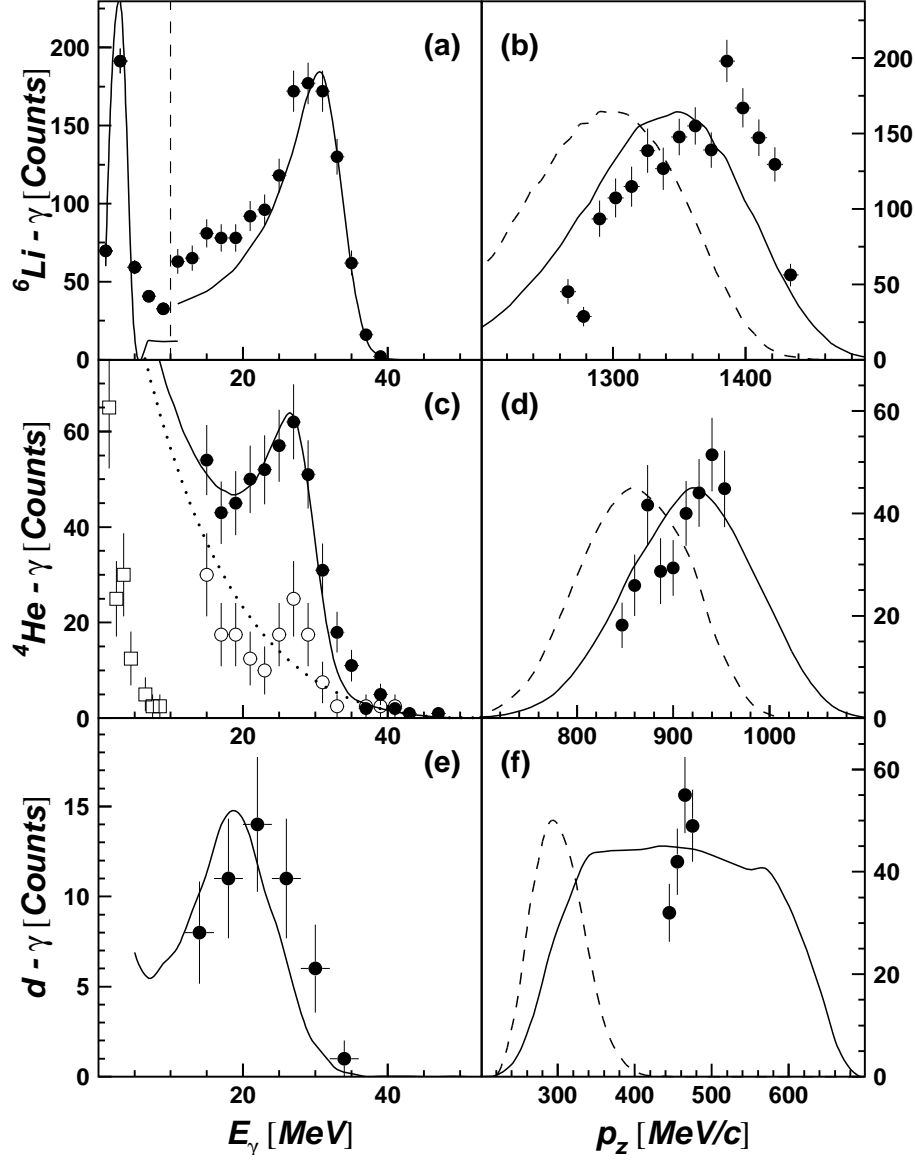


FIG. 6. Gamma-ray energy spectrum in the ${}^6\text{He}+p$ c.m. and momentum distribution of the coincident fragment for ${}^6\text{Li}$ (upper), α particles (middle) and deuterons (lower panel). The lines correspond to calculations of QFC on the ${}^5\text{He}$ cluster, the α core and one halo neutron, respectively; on the right with/without (solid/dashed) fragment FSI (see text). The distribution in (a) was divided by 3 below 10 MeV, and the open symbols in (c) are from an analysis investigating the rôle of the neutron background arising from breakup of ${}^6\text{He}$ (see ref. [23]).

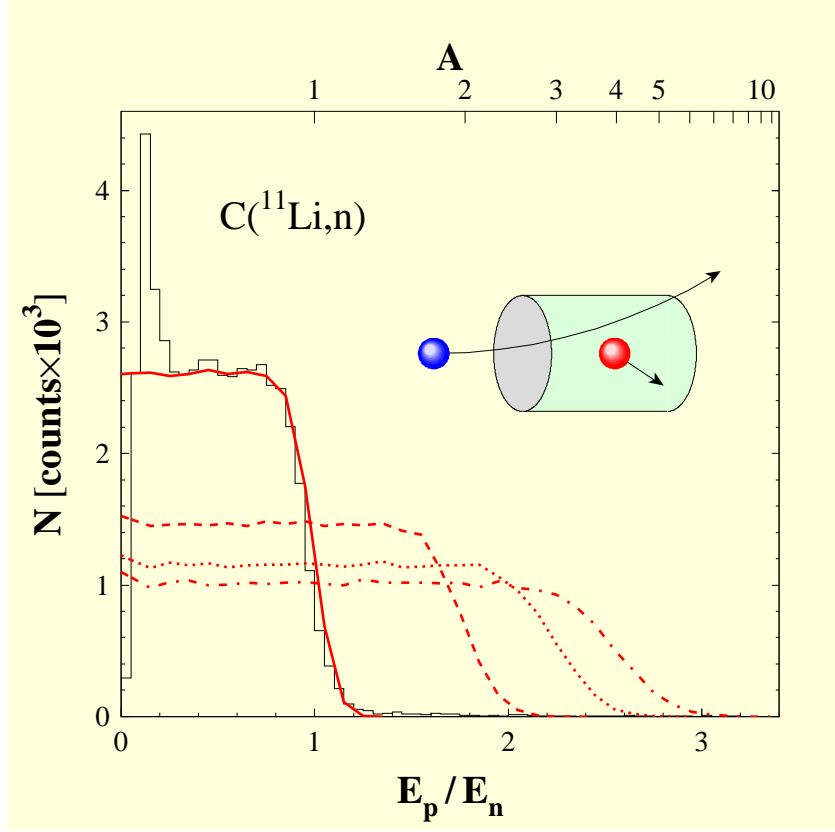


FIG. 7. E_p/E_n for $A=1$ (solid line), 2 (dashed), 3 (dotted) and 4 (dot-dashed). In the case of $A=1$, comparison is made to single neutron events from the ^{11}Li breakup of ^{11}Li . The excess of events at low E_p/E_n arise from reactions on the carbon component of the scintillator. From ref. [13]

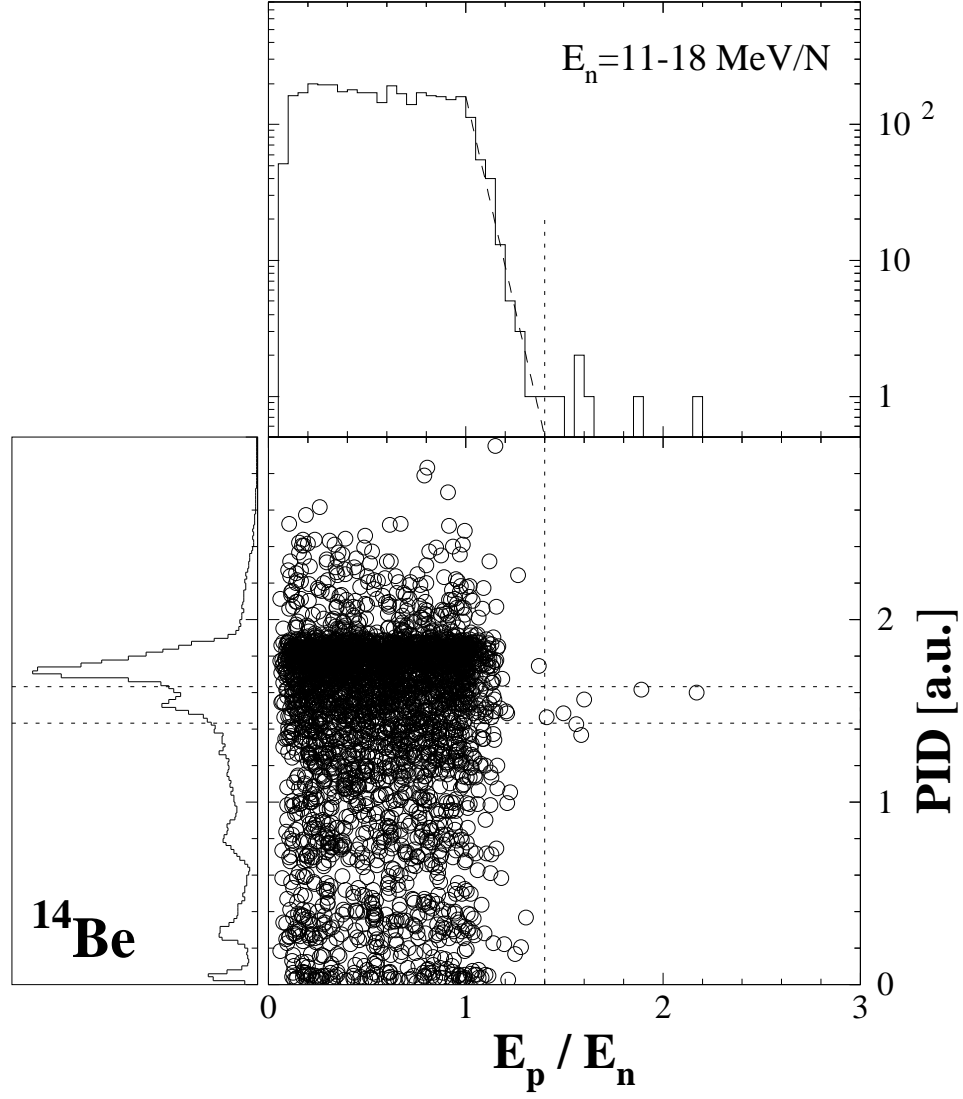


FIG. 8. PID versus E_p/E_n for the reaction ($^{14}\text{Be}, X+n$). The prominent peak at $\text{PID} \sim 1.7$ corresponds to ^{12}Be fragments. The horizontal band (dotted line) corresponds to the range of PID values encompassing the ^{10}Be fragments. From ref. [42].

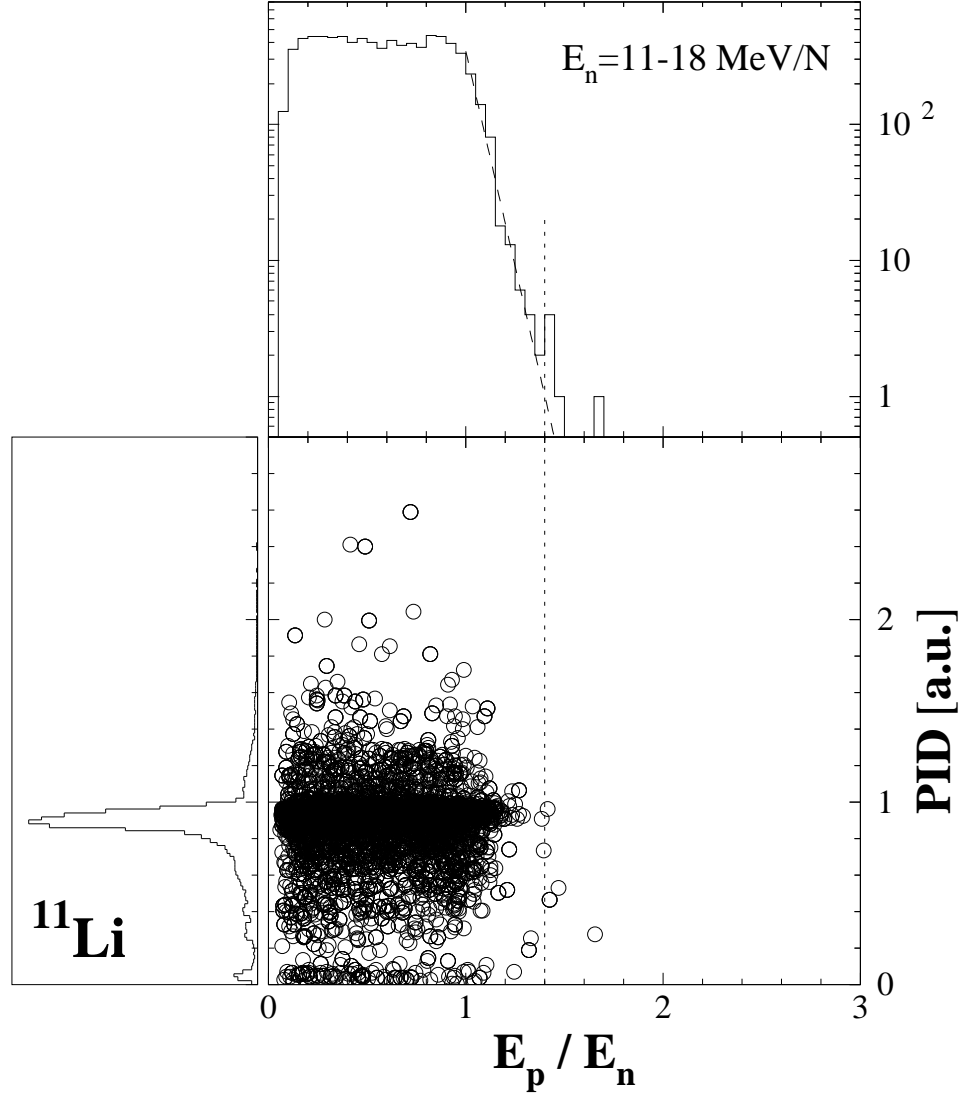


FIG. 9. PID versus E_p/E_n for the breakup of ^{11}Li . The prominent peak at $\text{PID} \sim 9$ corresponds to ^9Li fragments (see, ref. [42]).

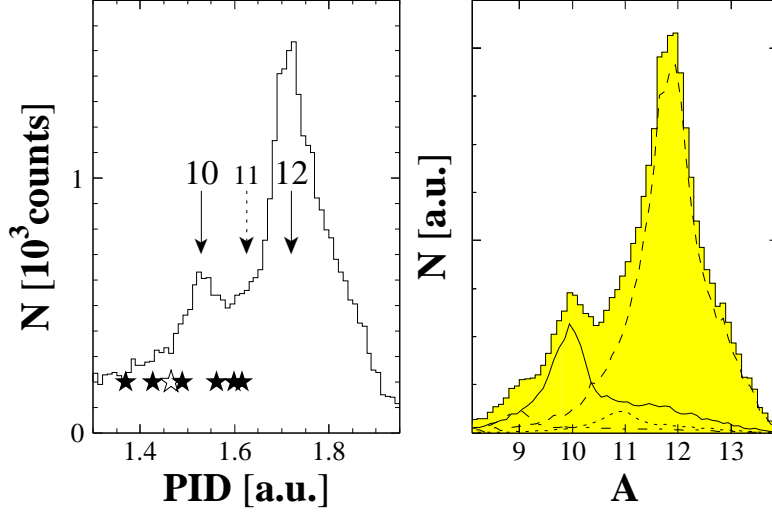


FIG. 10. Left: detail of the particle identification spectrum around $^{10,12}\text{Be}$ for the data from the reaction ($^{14}\text{Be}, \text{X}+\text{n}$); the 7 events with $E_p/E_n > 1.4$ are denoted by the symbols. Right: results of a simulation of the reactions ($^{14}\text{Be}, ^{9-12}\text{Be}$) in the target and telescope; the shaded histogram is the sum of the contributions from all four fragments (see, ref. [42]).

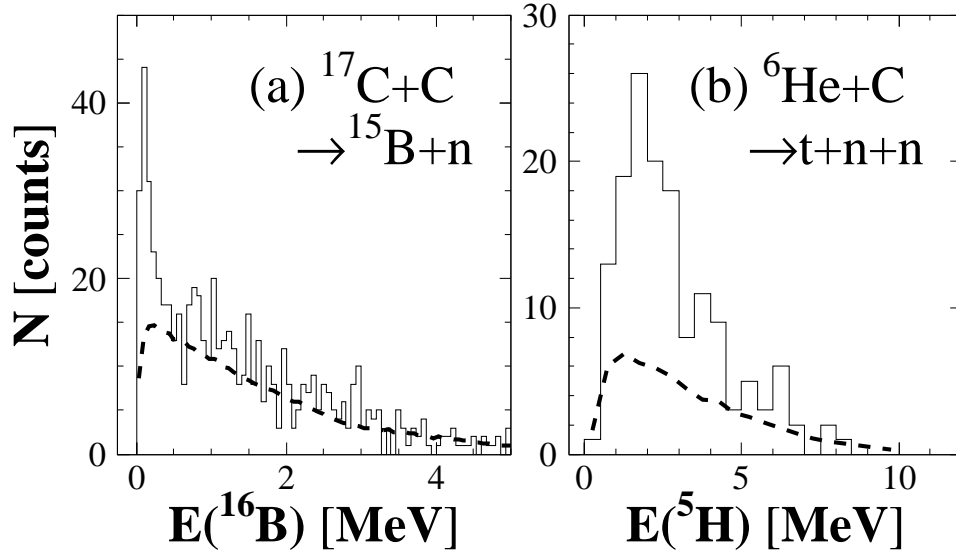


FIG. 11. Decay energy spectra for (a) $^{15}\text{B}-\text{n}$ [21] and (b) $t-\text{n}-\text{n}$ coincidences [50] for single-proton removal reactions. In both cases the reconstructed decay energy spectra are compared to that expected for uncorrelated events (dashed line) as generated via event mixing [21].